

# Rotational modulation of the ultraviolet line fluxes from the RS CVn star II Pegasi

L.M. Sarro<sup>1,2</sup> and P.B. Byrne<sup>1</sup>

<sup>1</sup> Laboratorio de Astrofísica Espacial y Física Fundamental (LAEFF) INTA, P.O. Box 50727, 28080 Madrid, Spain

<sup>2</sup> Armagh Observatory, Armagh BT61 9DG, N. Ireland

Received 30 July 1999 / Accepted 15 December 1999

**Abstract.** The exceptional in-orbit performance of the International Ultraviolet Explorer (IUE) for more than eighteen years has made it possible to accumulate an invaluable database of ultraviolet observations of a wide variety of objects and, in particular of active stars. Byrne et al. (1998) –hereafter Paper I– have presented a multiwavelength campaign of observations of the RS CVn star II Peg, partially based on one of the latest series of IUE spectra of this system. Here we investigate issues raised in Paper I such as the rotational modulation of chromospheric and transition region line fluxes and the long-term trends in the ultraviolet emission during the operational period of the instrument, the definition of a mean quiescent state and the changes operated in the radiative output by the occurrence of the most energetic flare detected in this star. We also perform a differential emission measure analysis based on the emission line fluxes and construct empirical models of the atmosphere of this star.

**Key words:** stars: activity – stars: individual: II Peg – stars: late-type – stars: variables: general – ultraviolet: stars

## 1. Introduction

Chromospheric and coronal heating on the Sun is highly concentrated into localised active regions of enhanced magnetic field. The distribution of such active regions with solar longitude is highly non-uniform, with the global brightness in high-temperature spectral features sometimes being dominated by a few very active regions. This is especially true near the maximum of the solar magnetic cycle.

Chromospherically active late-type stars exhibit most of the characteristics of the active Sun but on a globally much enhanced scale. RS CVn stars are close late-type binaries in which one component lies above the main sequence and, forced into corotation, is chromospherically active as a result of dynamo generated magnetic fields. RS CVn's exhibit a wide range of solar-like activity phenomena. These include non-radiatively heated chromospheres and X-ray emitting coronae (Doyle et al. 1992a; Doyle et al. 1992b), cool surface spots (Byrne 1992a; Byrne 1992b) and frequent flares (Doyle et al. 1989b).

Based on the solar experience, it might be expected that non-uniform distributions of magnetic heating in RS CVn stars would lead to variability in the stellar fluxes in suitable chromospheric and coronal lines as the star rotates, i.e. rotational modulation. Such effects have been very elusive, however, in spite of much observational effort (Rodonó et al. 1987; Byrne et al. 1987; Byrne et al. 1989; Doyle et al. 1989b; Doyle et al. 1989a). However, since most previous efforts have been based on either sampling a single rotation of the active star, or random sampling during many different rotations, there is an obvious risk of any rotational modulation being masked by short-term variability, such as flaring, or longer-term variations, such as the growth and decay of active regions.

In this paper we describe observations of the 6.72d period SB1 RS CVn K2IV binary, II Peg with the *IUE* satellite. High and low resolution spectra were taken during two stellar rotations in order to examine the above mentioned issues. Note that, as in Paper I, we use the orbital ephemerides of Vogt (1981), i.e.  $JD = 2443033.47 + 6.72422E$ , which we found according to Byrne et al. (1995) to be more accurate than any of the other published ephemerides. We also assume that the axial rotation of II Peg is tidally locked to the orbital motion of its companion.

## 2. Observations

The observations analysed here were obtained with the *IUE* short and long wavelength cameras (SWP and LWP respectively Boggess & Wilson 1987) during 12 consecutive days in September 1992. Several spectra were obtained each day alternating between LWP high resolution and SWP low resolution. A detailed list of observing dates, image numbers and line fluxes at Earth for the most prominent emission lines in each spectrum was included in Paper I as well as a complete description of the observing scheme and the reduction procedure.

## 3. Results

### 4. The “quiescent” spectrum of II Peg

#### 4.1. SWP line fluxes (1200–2000 Å)

As it was previously discussed (see e.g. Doyle et al. 1989b), active RS CVn stars like II Peg flare frequently. These flares are

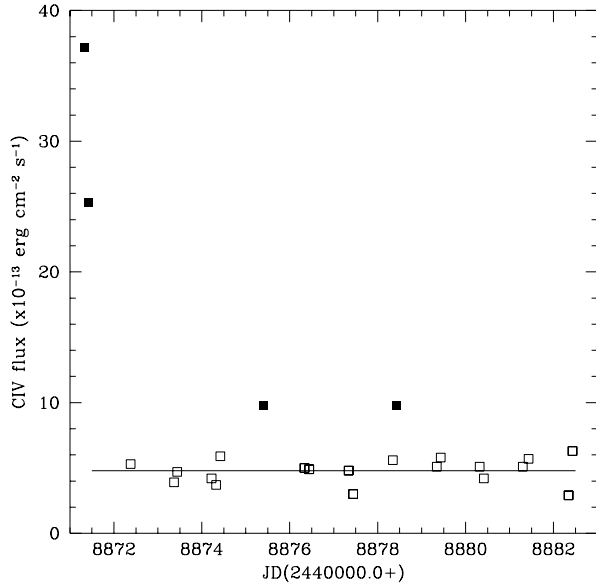


**Fig. 1.** The *open symbols* represent CIV  $\lambda 1548/51\text{\AA}$  fluxes measured from *IUE* SWP LORES spectra of II Peg taken during the period 5–16 September 1992. The *filled squares* are those flux measurements during which we believe flares were taking place. The horizontal line is the proposed mean “quiescent” flux of II Peg at this epoch.

detected in *IUE* SWP spectra by dramatic but temporary increases in the flux of all emission lines but they are especially obvious in those of the CIV doublet ( $\lambda 1548/51\text{\AA}$ ). Before discussing other possible types of variability we will study the evidence for flaring which are present in the data.

In Fig. 1 we show the sequence of measured CIV fluxes as a function of the Julian date. The two consecutive flux values recorded on spectra SWP45531 and SWP45532 (at the left of the graph) are obviously very much higher than the mean of the remaining values. In fact, their fluxes are  $18.75\sigma$  and  $11.7\sigma$  respectively above the mean value computed excluding these two fluxes. The probability of getting two deviations of this size in normally distributed values is vanishingly small. Accordingly we treat these two flux values as flares.

Without SWP45531 and SWP45532 the new mean CIV flux is  $5.28 \times 10^{-13} \text{erg cm}^{-2} \text{s}^{-1}$  with a standard deviation of  $1.71 \times 10^{-13} \text{erg cm}^{-2} \text{s}^{-1}$ . With these new values two further spectra stand out as having anomalously large values, i.e. those of SWP45586 and SWP45618 (the two solid squares near the centre of Fig. 1), each  $5.4\sigma$  from the new mean excluding them. Again it is reasonable to suspect that they too are flares and we will treat them as such. We propose to treat those flux values outside of these individual flares (open squares in Fig. 1) as “quiescent” values.

There has been controversy over the years about the ability of *IUE* to detect weak features. Essentially this revolves around the question of “flat fielding” the complicated detector system and the repeatability of that process. Ayres (1990) has concluded that, taking all sources of error into account, the ability of *IUE* to detect weak, unresolved emission lines at a level of  $3\sigma$  with its SWP LORES camera in spectra of 50–100 min exposure

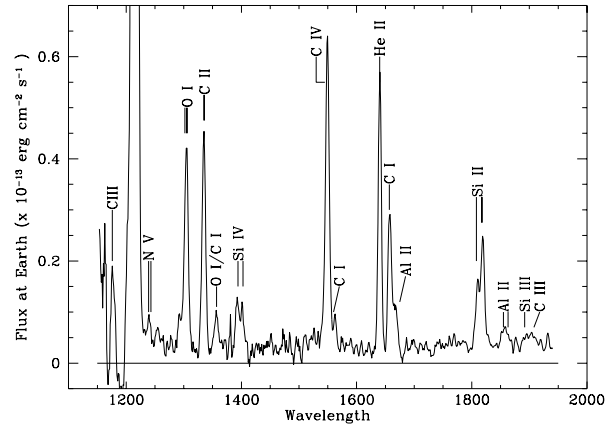


**Fig. 2.** The mean “quiescent” *IUE* SWP LORES spectrum of II Peg taken during the period 5–16 September 1992. The *horizontal line* is the zero flux level. Some prominent emission lines discussed in the text are labelled.

**Table 1.** Mean quiescent SWP line fluxes.

Ion	$\lambda$ $\text{\AA}$	Line Flux at Earth $\times 10^{-13} \text{erg cm}^{-2} \text{s}^{-1}$	Other lines?
CIII	1176	1.5	
NV	1241	0.25	
CI	1253	0.2	SiII?
SiIII	1299	0.6	SiI?
OI/CI	1357	0.5	MgIV?
SiIV	1394	1.9	OIV
CI	1560	0.4	
AlIII	1855/63	0.8	
SiIII]	1892	0.3	
SI	1900	0.2	
CIII]	1908	0.4	

is  $\sim 6 \times 10^{-14} \text{erg cm}^{-2} \text{s}^{-1}$ . He furthermore pointed out that co-adding separate spectra increases the signal-to-noise of the resulting spectrum by  $\sqrt{N}$ , where  $N$  is the number of spectra.

With this in mind we have formed an average SWP spectrum using all the SWP spectra except those positively identified above as flares, i.e.  $N=19$ . Note that, before preparing this mean all of the spectra were adjusted in wavelength so that the singlet HeII  $\lambda 1640\text{\AA}$  line in each spectrum was centred on the laboratory wavelength. This was done to overcome any shifts in wavelength scale caused by imperfect centering of the star on the spectrograph entrance aperture, which in *IUE* has an appreciable inclination to the direction perpendicular to the dispersion. The result is given in Fig. 2.

Referring to the results of Ayres (1990) we expect a  $3\sigma$  detection limit in the mean spectrum of  $6 \times 10^{-14} \sqrt{19}$ ,  $\sim 1.4 \times 10^{-14} \text{erg cm}^{-2} \text{s}^{-1}$ . The mean spectrum shown in Fig. 2 was examined for features exceeding this limit. All wavelengths at which we believe lines are present are listed in Table 1 and indicated on Fig. 2. The flux in each of these features was derived by fitting gaussians of FWHM equal to the resolution of the spectrograph. The central wavelengths of these fits were

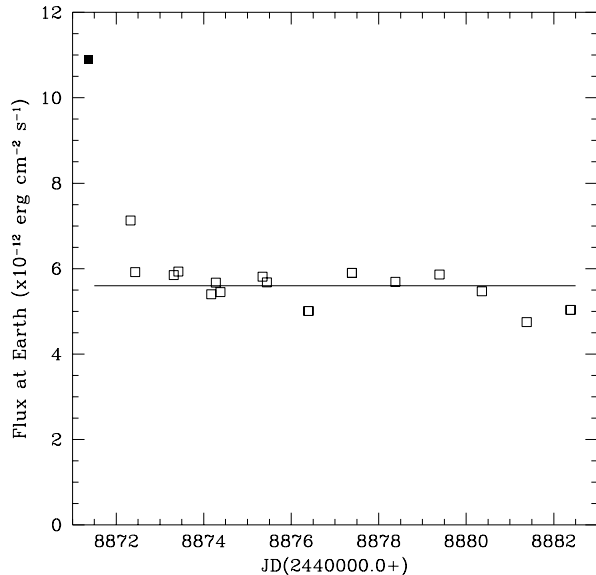


**Fig. 3.** The *open squares* represent Mg II  $k$   $\lambda 2795.5\text{\AA}$  fluxes measured from *IUE* LWP HIRES spectra of II Peg taken during the period 5–16 September 1992. The *solid square* is the flux measurement during which we believe a flare was taking place. The horizontal line is the proposed mean “quiescent” flux of II Peg at this epoch.

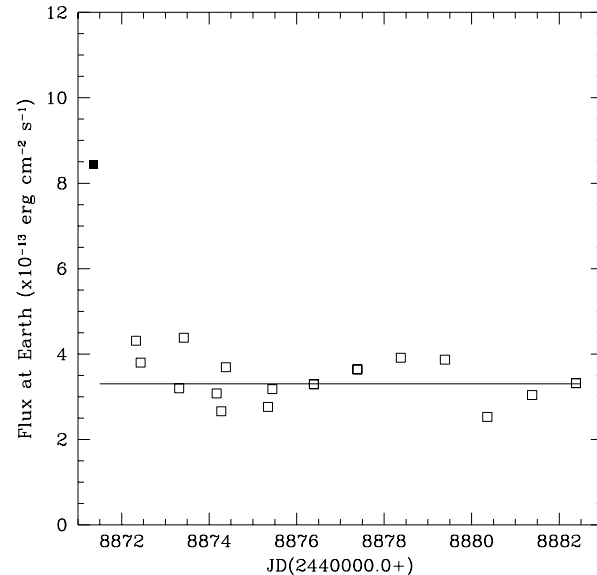


**Fig. 4.** The *open squares* represent Fe II  $\lambda 2625.7\text{\AA}$  fluxes measured from *IUE* LWP HIRES spectra of II Peg taken during the period 5–16 September 1992. The *solid square* is the flux measurement during which we believe a flare was taking place. The horizontal line is the proposed mean “quiescent” flux of II Peg at this epoch.

then compared with the atlas of the solar spectrum in the same region Brekke (1993). These proposed identifications and the measured fluxes are also given in Table 1.

Note, however, that there is a considerable amount of residual flux between the lines identified as discrete features in the tables. It seems unlikely that this could be due to photospheric continuum from the late-type primary of the system. There is no evidence of breaks in its distribution at the wavelengths of the Si I continua (at  $\lambda 1524\text{\AA}$  and  $\lambda 1682\text{\AA}$ ), making an origin therein unlikely as suggested by Phillips et al. (1992) for the flaring state of II Peg. These may be due to the superposition of many weaker lines which, at this resolution, cannot be individually recognised.

How justified are we in treating these resulting fluxes as “quiescent”? The CIV doublet is the best exposed line in the quiescent spectra. Its mean flux is  $4.80 \times 10^{-13} \text{erg cm}^{-2} \text{s}^{-1}$  with a standard deviation of  $0.92 \times 10^{-13} \text{erg cm}^{-2} \text{s}^{-1}$ . Within the measurements constituting this mean, however, there is still a factor of 2.2 variation between the extreme values ( $2.9 \times 10^{-13} \text{erg cm}^{-2} \text{s}^{-1}$  and  $6.3 \times 10^{-13} \text{erg cm}^{-2} \text{s}^{-1}$ , respectively). In view of Ayres’ conclusions, it seems unlikely that this “non-flare” spectrum is truly quiescent.

#### 4.2. LWP line fluxes (2000–3000 Å)

As with the SWP spectra we show in Fig. 3 the variation of the essentially chromospheric Mg II  $k$  line. One value (solid square) is clearly higher than all of the others. This spectrum (LWP23854) was bracketted in time by the two SWP spectra showing the large CIV flare. The slightly hotter Fe II lines near  $\lambda 2620\text{--}30\text{\AA}$  whose time behaviour is shown in Fig. 4, are also

clearly elevated at this time. Accordingly we consider it to be affected by a flare too.

A second point (that derived from LWP23864) is also high in Mg II  $k$ . This spectrum was one of a pair of LW spectra taken on JD2448872 about 2.5 hr apart. The following spectrum, LWP23865, shows no evidence of enhanced flux. There was an intervening SWP spectrum (SWP45543) of 100 min duration which shows no clear evidence of flare activity in CIV. The slightly hotter Fe II  $\lambda 2625.7\text{\AA}$  line is not elevated above the mean value. CIV flares tend, however, to be more short-lived than those in chromospheric lines. Furthermore, the Mg II  $h$  line is close to the overall mean value. Therefore, there seems to be no good reason to omit this spectrum from determining the overall mean “quiescent” flux in the LWP lines.

#### 4.3. Rotational modulation of line fluxes

One of the most striking characteristic of the RS CVn stars as a class is the rotational modulation of their visible light due to the presence of large scale cool starspots (see e.g. Byrne 1992a or Byrne 1992b). Whether chromospheric line emission undergoes a similar modulation is an unresolved issue (see e.g. Rodonó et al. 1987; Andrews et al. 1988; Doyle 1988 or Doyle et al. 1989a). Our data set, providing regular monitoring of line fluxes ranging from the chromosphere to the mid-transition region, is well suited for examining this issue.

In Figs. 5 and 6 we show some of the main chromospheric and transition region line fluxes plotted against rotational phase. It is clear in Fig. 6 that there is no evidence of systematic rotational modulation in the transition region lines from CII  $\lambda 1335/6\text{\AA}$  ( $\log T_{\text{eff}} \sim 4.5$ ) to CIV  $\lambda 1548/51\text{\AA}$  ( $\log T_{\text{eff}} \sim 5.0$ ).

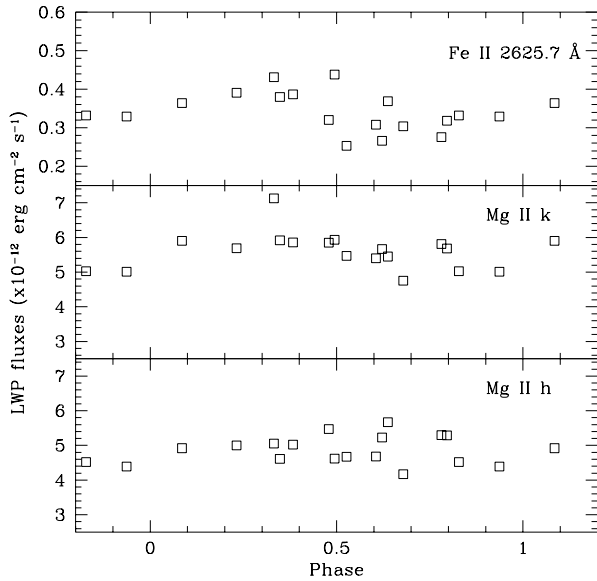


**Fig. 5.** The “quiescent” *IUE* LWP emission line fluxes of II Peg taken during the period 5–16 September 1992 vs. rotational phase (from Vogt, 1981).

The chromospheric lines in Fig. 5, on the other hand, show hints of such a modulation, albeit with considerable scatter about the mean trend. Fe II  $\lambda 2625.7\text{\AA}$ , in particular, shows evidence of a modulation with a peak-to-peak amplitude of  $\sim 30\%$  about the mean, the maximum being about phase,  $\varphi \approx 0.4$  and minimum at about  $\varphi \approx 0.6$ . A quantitative assessment of the influence of rotation on the line fluxes can be obtained by fitting the data with constant and sinusoidal functions and comparing the  $\chi^2$  values of the fits. This analysis shows how the decrease in the total error is only significant (above 5%) in the low transition region lines of C II (17%) and O I (26%) compared to a 48% in the Mg II h line, 5% in the Mg II k line and 44% in the Fe II lines.

#### 4.4. Comparison with previous results

II Peg is one of the most intensively monitored RS CVn systems with *IUE*. Therefore we have the opportunity to compare our results with those of previous epochs. We have searched in the literature for previous determinations of the mean quiescent fluxes of the stronger lines in both the SWP and LWP ranges. These are summarized in Table 2 and Fig. 7.

Note first of all that our present fluxes are comparable to those derived by previous authors. However, our values are among the *lowest* recorded in the transition region lines, C II  $\lambda 1335/6\text{\AA}$ , CIV  $\lambda 1548/51\text{\AA}$  and He II  $\lambda 1640\text{\AA}$  but second *highest* in the Mg II  $\lambda 2796/803\text{\AA}$  doublet.

As part of an investigation of the long-term variability of the ultraviolet emission of II Pegasi, the C IV flux for each image in the *IUE* archive was measured. All spectra, including those corresponding to the 1992 observing campaign, were obtained from the *IUE* Final Archive at <http://archive.stsci.edu/iue> and extracted using NEWSIPS Nichols & Linsky (1996) so the

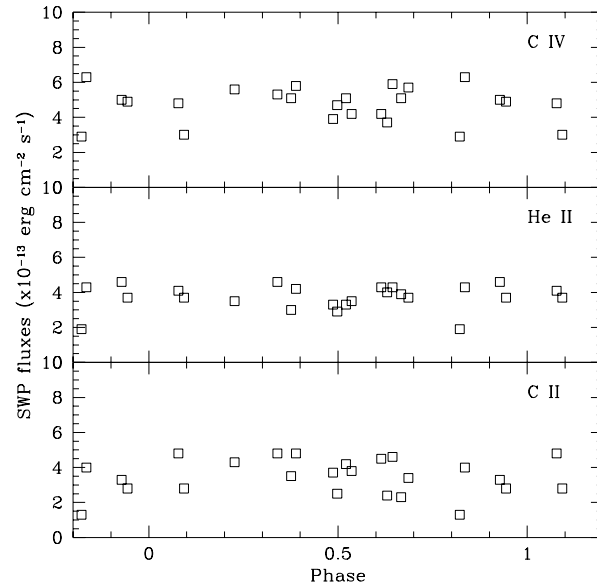


**Fig. 6.** The “quiescent” *IUE* SWP emission line fluxes of II Peg taken during the period 5–16 September 1992 vs. rotational phase (from Vogt, 1981).

**Table 2.** Mean quiescent line fluxes at Earth for some of the strongest lines in the ultraviolet spectrum of II Peg in 1992 compared to published values at previous epochs.

Year	Line Fluxes at Earth			
	CII $\lambda 1335/6\text{\AA}$	CIV $\lambda 1548/51\text{\AA}$	HeII $\lambda 1640\text{\AA}$	MgII $\lambda 2796/803\text{\AA}$
	$\times 10^{-13} \text{erg cm}^{-2} \text{s}^{-1}$			
1979 <sup>a</sup>	4.7	6.7	4.3	92.2
1980 <sup>b</sup>	6.4	9.3	7.3	85.6
1981 <sup>c</sup>	4.3	9.5	4.5	92.4
1983 <sup>d</sup>	4.6	8.6	5.5	102.4
1984 <sup>e</sup>	—	—	—	105.4
1985 <sup>f</sup>	3.7	8.4	4.9	115.8
1986 <sup>g</sup>	3.4	6.2	3.5	98.4
1989 <sup>h</sup>	4.5	6.8	4.0	102.0
1990 <sup>i</sup>	5.2	9.4	5.5	105.7
1992 <sup>j</sup>	3.6	4.8	3.7	105.7

<sup>a, b</sup> quoted in Doyle et al. 1989a; <sup>c</sup> Rodonó et al. 1987; <sup>d</sup> Andrews et al. 1988; <sup>e</sup> Byrne et al. 1989; <sup>f</sup> Doyle, 1988; <sup>g</sup> Doyle et al. 1989a; <sup>h</sup> Doyle et al. 1992a; <sup>i</sup> Doyle et al. 1993; <sup>j</sup> Present work

fluxes presented here do not necessarily coincide with the fluxes derived by the original observers. The results are presented in Fig. 8 where flares identified in the bibliography and poor signal to noise spectra have not been included. Despite the scatter of data points within each observing run, hints of some kind of modulation can be identified as a decrease in the mean fluxes between JD2445000 and JD2447000 and a non-monotonic increase thereafter. The most recent observations in the plot correspond to JD2450371 (October 1996) and were taken with the Goddard High Resolution Spectrograph on board HST.

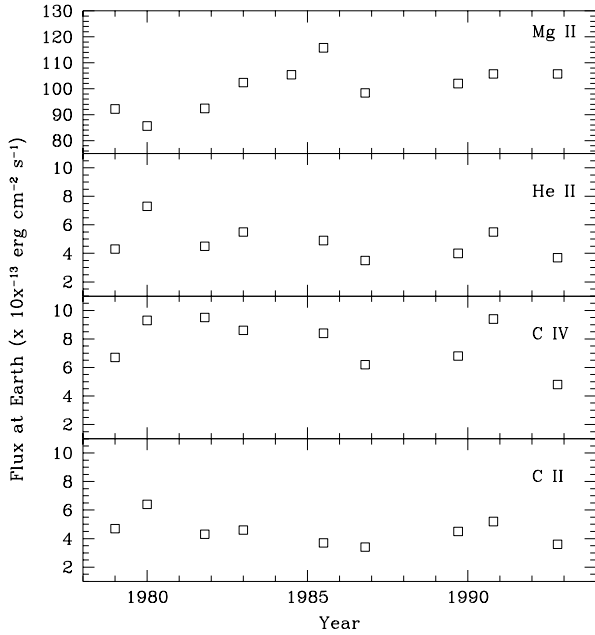


**Fig. 7.** The mean “quiescent” *IUE* emission line fluxes of II Peg taken over the years 1979–92.

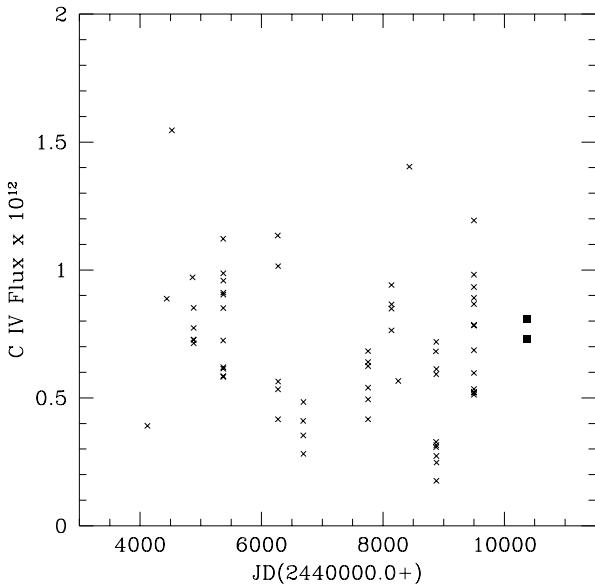


**Fig. 8.** C IV line fluxes re-extracted from the *IUE* Final Archive as a function of the Julian Date. Crosses represent individual fluxes measured by the authors on archived *IUE* spectra, solid squares correspond to C IV fluxes from *HST* GHRS observations taken in 1996 and extracted from the *HST* archive and solid circles correspond to the mean values quoted in Table 2.

## 5. Flare line fluxes

### 5.1. SWP line fluxes (1200–2000 Å)

As we have concluded in Sect. 4.1, there is evidence for at least 2 separate flares in the spectra of II Peg. In Fig. 12 we show the individual spectra of these flares compared to the mean “quiescent” spectrum derived from the non-flare spectra. Apart from

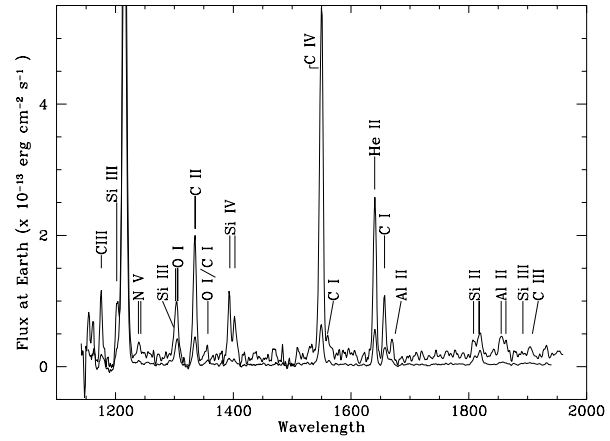


**Fig. 9.** The SWP 45531 flare spectra compared to the mean “quiescent” spectrum of II Peg. Individual spectral lines are identified on the top spectrum.

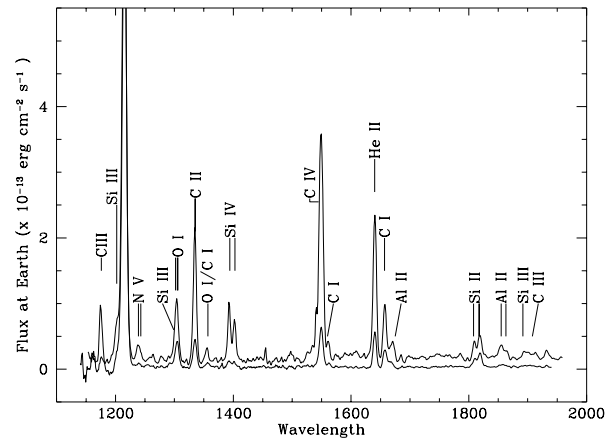


**Fig. 10.** The SWP45532 flare spectra compared to the mean “quiescent” spectrum of II Peg. Individual spectral lines are identified on the top spectrum.

the dramatic increases in the line fluxes there is also evidence for a continuum, or, perhaps, a large number of unresolved weak lines between the most conspicuous ones.

Flares are generally expected to occupy a relatively small fraction of the stellar surface area. Therefore, to a good approximation, we can treat the quiescent atmosphere as unaffected by the flare and forming an additive background to the line flux from the flares themselves. We have therefore subtracted the mean quiescent fluxes in each detected line from those fluxes measured during the flares. The resulting net fluxes will be treated as a signal purely from the flares themselves.

As we have pointed out above, we see evidence of a continuous flux distribution underlying those individual lines. It is possible that there is a contribution to this “continuum” from unresolved individually weak lines. We have unsuccessfully searched for evidence of the Si I continuum breaks at  $\lambda 1524\text{\AA}$  and  $\lambda 1682\text{\AA}$  as suggested by Phillips et al. (1992). In the absence of firm evidence either way we will treat the distribution of radiation as a true continuum extending over the entire SWP wavelength range as has been suggested by other authors (see

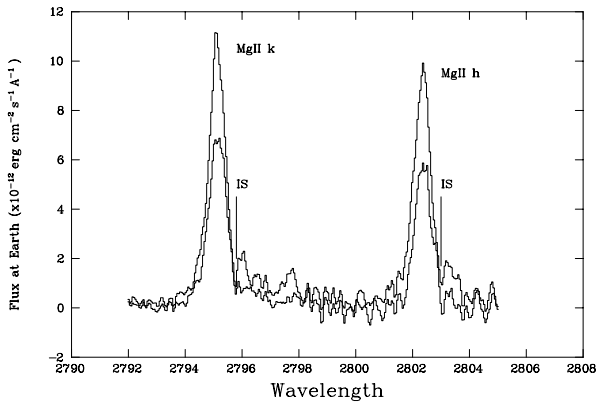


**Fig. 11.** A sample “quiescent” *IUE* LWP HIRES spectrum of II Peg (LWP23864) in the neighbourhood of the Mg II h&k lines. Overplotted is the large flare of 5 September 1992 (LWP23854). The vertical lines marks the position of the interstellar lines (IS).

Byrne 1996 and references therein). We have also measured the 1595 Å continuum power as defined in Phillips et al. (1992) and confirmed the relationship between this ‘continuum’ and the C IV line power. Our spectra yield C IV line powers of 28.06 and 27.86 for SWP45531 and SWP45532 respectively and ‘continuum’ powers of 28.08 and 27.89, all measurements in logarithmic units.

### 5.2. LWP line fluxes (2000–3000Å)

Only one LWP HIRES spectrum was taken during a flare namely LWP23854. This was obtained in between the two SWP flare spectra on the night of 5 September (SWP45531 and SWP45532). In this spectrum all the observed emission lines are dramatically enhanced in flux and considerably broadened (Fig. 11).

Assuming, as we did for the SWP spectra in Sect. 5.1, that the flare was confined to a limited area of the disk and that the global flux was largely unaffected by the flare, we have subtracted LWP23864 (the post-flare, quiescent line profile) from the flare line profile. This is shown in Fig. 12

Analysing a less energetic flare, Doyle et al. (1989b) detected in the excess emission from the flare two absorption features on both sides of the Mg II k line maximum. The origin of the red one is clear (it is the interstellar absorption line also found in our data) while the blue one could be attributed, according to the authors, to an erupting filament moving at a speed of 25 km s<sup>-1</sup> relative to the bulk of the flare. In our data we do not find such clear evidence for overlying cold material absorbing the emission from the flare, but we still detect traces of these kind of spectral features. In particular, the ones marked in Fig. 12 show similar velocities in both lines (roughly 45 km s<sup>-1</sup>) measured relative to the maximum emission in the flare spectrum.

### 5.3. Differential emission measure

Following Jordan et al. (1987) we have constructed emission measure curves for those spectra with measurable Si III] λ

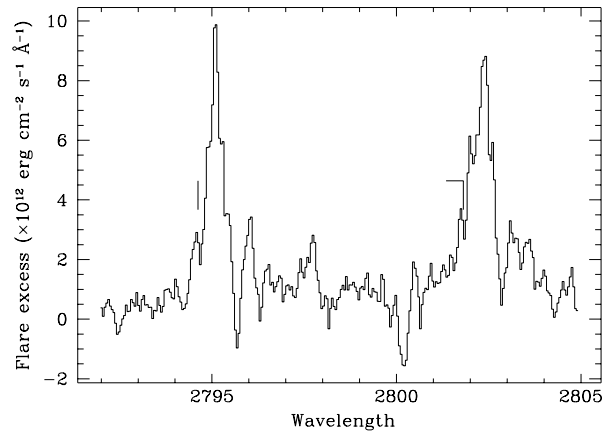


**Fig. 12.** The LWP line profiles for the flare spectrum (LWP23854) after subtraction of LWP23864 (“quiescent” spectrum).

1892 Å line fluxes, namely, the mean quiescent spectrum and the flare spectrum SWP45532. This intersystem line was used to estimate the electron density as described in Sect. 5.4. Solar abundances were adopted given the lack of estimates of transition region abundances for this RS CVn system. Only recently, Mewe et al. (1997) using ASCA spectra of II Pegasi found an underabundance of silicon of a factor 5 relative to the cosmic abundances of Anders & Grevesse (1989) used in this paper (they found other non-solar abundances of elements not relevant to our emission measure analysis). As shown below, the emission measure curve obtained with solar abundances is relatively smooth and such a change in the silicon abundance would significantly increase the scatter in the data. In order to use the new abundances in the emission measure computation we would need carbon and nitrogen abundances obtained consistently (i.e. fitting an ASCA spectrum) something which was not possible with the dataset analysed in Mewe et al. (1997).

In the emission measure formalism we have also used the equilibrium ion populations of Arnaud & Rothenflug (1975), and the collisional strengths included in Table 4. The results are shown in Figs. 13 and 14.

These results can be compared with previous determinations of this emission measure distribution, in particular with the latest reexamination of the *IUE* observations of this RS CVn system. In the work by Griffiths & Jordan (1998) based on observations of II Pegasi taken in October 1981, a slightly different definition of the emission measure (apparent volume emission measure) is used which merely introduces a new geometric scaling factor. Once this is taken into account, the main differences affect the absolute value of the emission measure and the shape of the temperature dependence. The absolute value of the logarithmic emission measure for the data obtained in 1992 is lower by a factor  $\approx 0.3$  at  $\log T_e = 5.0$  due to the considerably lower value of the C IV line flux. Given that our transition region line fluxes are amongst the lowest ever measured, this means that similar conclusions could be drawn by comparison with any other dataset. The ratio of the 1981 line fluxes to the 1992 measurements increases with increasing line formation temper-

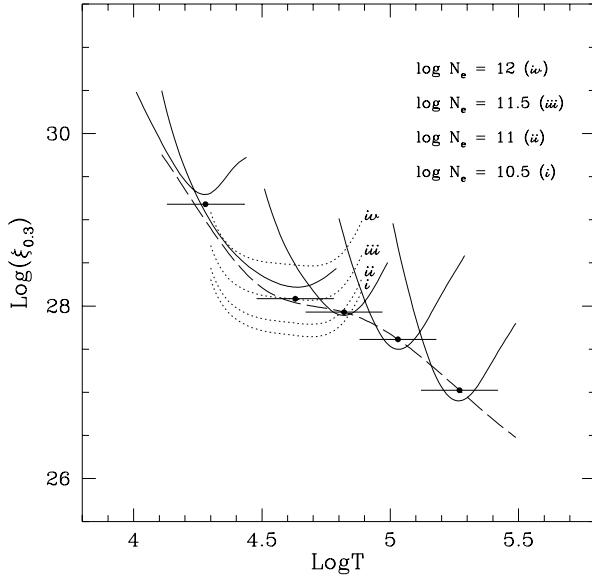


**Fig. 13.** Logarithmic emission measure diagram for the mean quiescent spectrum of II Pegasi. Solid lines represent the emission measure loci computed (from left to right) with the Si II, C II, Si IV, C IV and N V line fluxes. Dotted lines correspond to the emission measure loci of the Si III] intersystem line assuming four different electron densities. The dashed line is the fit to the emission measure curve.

**Table 3.** Line fluxes at Earth for some of the strongest lines in the SW ultra-violet spectrum of II Peg in 1992 during flares after subtraction of the mean “quiescent” fluxes in the same lines. \* marks lines with low signal to noise ratio.

Line	Mean Quiet	Line Flux at Earth			
		531	532	586	618
$\times 10^{-13} \text{erg cm}^{-2} \text{s}^{-1}$					
CIII $\lambda$ 1176 $\text{\AA}$	1.5	4.8	4.2	–	3.0
NV $\lambda$ 1239/43 $\text{\AA}$	0.25	1.25	1.65	–	–
OI $\lambda$ 1302/5/6 $\text{\AA}$	3.3*	3.6*	3.4*	–	1.5*
SiIII $\lambda$ 1299 $\text{\AA}$	0.6*	–	–	–	–
CII $\lambda$ 1335/6 $\text{\AA}$	3.1	9.0	9.1	1.2	2.6
OI/CII $\lambda$ 1357 $\text{\AA}$	0.5	–	–	–	–
SiIV $\lambda$ 1394 $\text{\AA}$	1.0	4.2	3.7	2.0	2.5
SiIV $\lambda$ 1403 $\text{\AA}$	0.9	3.1	2.7	1.6	1.8
CIV $\lambda$ 1548/51 $\text{\AA}$	4.9	32.2	20.4	5.0	5.0
HeII $\lambda$ 1640 $\text{\AA}$	3.7	11.7	11.3	2.9	1.4
CII $\lambda$ 1657 $\text{\AA}$	2.5	2.8	3.1	–	0.8
SiIII $\lambda$ 1808 $\text{\AA}$	1.0	1.25	1.1	0.7	0.5
SiIII $\lambda$ 1817/8 $\text{\AA}$	1.6	1.7	1.4	1.5	0.9
AlIII $\lambda$ 1855/63 $\text{\AA}$	0.8*	–	–	–	–
SiIII $\lambda$ 1892 $\text{\AA}$	0.3*	–	0.7*	–	–
CIII $\lambda$ 1908 $\text{\AA}$	0.4*	0.8*	0.3*	–	–

ature and, thus, the shape of the emission measure distribution changes. Above the Si IV formation temperature, this implies a steeper decrease of the emission measure distribution for our data. Although with a different definition of the emission measure and different atomic parameters, Byrne et al. (1987) constructed another emission measure distribution based on the

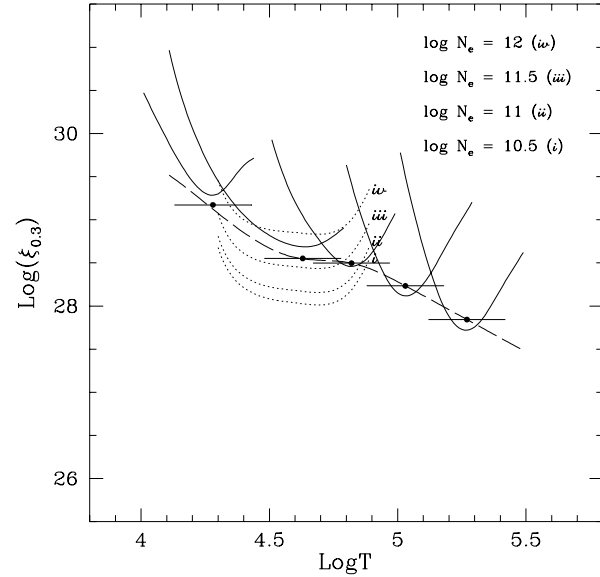


**Fig. 14.** As Fig. 13 but for the flare spectrum SWP45532.

**Table 4.** Atomic parameters used in the computation of the emission measure distribution.

Ion	$\lambda$	$\log T_e$	$\Omega$	$w_1$
N V	1239 $\text{\AA}$ + 1243 $\text{\AA}$	5.3	$7.2^6$	2
C II	1335 $\text{\AA}$ + 1336 $\text{\AA}$	$\simeq 4.2$	$6.2^{2,3}$	6
Si IV	1394 $\text{\AA}$ + 1403 $\text{\AA}$	4.83	$18.2^5$	2
C IV	1548 $\text{\AA}$ + 1551 $\text{\AA}$	5.04	$9.6^6$	2
Si II	1808 $\text{\AA}$ + 1817 $\text{\AA}$	$\simeq 4.1$	$15.2^1$	6
Si III	1892 $\text{\AA}$	4.5	$3.2^4$	1

[1] Mendoza (1981), [2] Hayes & Nussbaumer (1984),  
 [3] Lennon et al. (1975), [4] Baluja et al. (1980,1981),  
 [5] Dufton & Kingston (1985), [6] Cochrane & McWhirter (1983)

same line fluxes which they fitted with a power law. Another data set obtained in 1983 was analysed by Doyle et al. (1989b) in order to obtain emission measure curves for II Peg. Using the same methodology as in Byrne et al. (1987) they obtained emission measure curves with a similar behaviour in the temperature range  $4.8 < \log T_e < 5.3$  for the quiescent state while the flaring state showed a flattening of the distribution between the C IV and N V formation temperatures.

#### 5.4. Electron density

The density diagnostics available for the set of emission lines present in the SWP spectra were discussed in detail in Byrne et al. (1987). Following this discussion we have computed electron densities for the mean quiescent spectrum and the two flare spectra with good signal-to-noise in the lines involved in the analysis (namely, SWP 45531 and SWP45532) using the calibration of the Si IV( $\lambda$ 1394/1403)/C III( $\lambda$ 1909) line ratio against the quiet solar limb observations by Doschek et al. (1976). The Si IV total emission in the resonance doublet was computed from the  $\lambda$ 1394 component assuming the optically thin line ratio (2:1)

due to the blending of the weaker component at  $\lambda 1403$  with nearby O IV and S IV lines.

Under the assumptions underlying this calibration (solar abundances of carbon and silicon and formation temperature roughly equal for both lines) we have obtained a value of  $\log(P_e/k)=15.5$  for the quiescent state of II Peg and 15.7 and 16.0 for SWP 45531 and SWP 45532 respectively. These correspond to  $\log N_e=10.7$  in quiescence and  $\log N_e=10.9$  and  $\log N_e=11.2$  for the two flaring spectra.

As we mentioned in the previous section, the Si III]  $\lambda$  1892 Å line allows us to estimate the electron density by an indirect method. It consists in assuming different values of the electron density in the emission measure formalism and choosing the one that provides a smooth emission measure curve. Using this method we have obtained electron densities roughly equal to  $11.6\pm 0.25$  for the quiescent state and  $11.9\pm 0.25$  for the flare spectrum.

It is important to point out that the quiescent state electron density is in complete agreement with the density estimate obtained by Griffiths & Jordan (1998) despite the large difference in the radiative losses of II Peg in both epochs. If we gauge the radiative losses of the transition region of this system by adding up the Si IV, C IV and N V line fluxes, we find that in 1981 this amounts to  $2.76 \times 10^5$  erg cm<sup>-2</sup> s<sup>-1</sup>, roughly twice the value for quiescence in 1992. In fact, even within the data of Rodonó et al. (1987) we can find hints that the electron density estimated in this way is independent of the level of activity as measured by the radiative losses of the transition region of II Peg. In the series of papers following Rodonó et al. (1987) up to the work by Griffiths & Jordan (1998) a distinction is made between a quiet hemisphere (used for comparison above) and an active hemisphere on II Peg based on transition region fluxes and spot modelling (see Byrne et al. 1987). The ratio between the radiative losses of the transition region (measured in the same way as above) of the active hemisphere relative to the quiet hemisphere is roughly 5, but the ratio of the C II  $\lambda$  1335 Å flux to the Si III]  $\lambda$  1892 Å flux (that measures the relative position of the Si III] loci relative to the mean emission measure curve) is equal for both hemispheres.

The electron density estimate based on the Si III] loci is one order of magnitude higher than the one obtained with the Si IV( $\lambda\lambda$  1394/1403)/C III]( $\lambda$ 1909) line ratio. This can be partly due to the fact, already pointed out by Byrne et al. (1987), that a significant fraction of the Si III] is formed at temperatures below  $\log T_e = 4.5$ . But under the assumption of constant pressure in the transition region, this is still insufficient to account for the difference of one order of magnitude in the estimates. As a matter of fact, even if we assume a line formation temperature of  $\log T_e = 4.3$  for the Si III] line and  $\log T_e = 4.8$  for Si IV( $\lambda\lambda$  1394/1403) and C III]( $\lambda$ 1909) we find a change in density of only 0.5 dex.

This kind of discrepancy has already been pointed out for other stars (see Linsky et al. 1995) in the sense that density sensitive line ratios yield values systematically lower than emission measure based densities. Furthermore, densities obtained via density sensitive line ratios seem to cluster in a

narrow band around  $\log N_e = 10.0$  independent of activity level, spectral type or luminosity class (see Ayres et al. 1998; Wood et al. 1996 or Wood et al. 1997). These puzzling results suggest that the density stratification in the transition region is still a matter of debate. It has been proposed that the surface of active stars is covered by at least two types of regions with substantially different densities but similar emission measures. Although the present data do not allow further speculation, the fact that in II Pegasi in particular, emission measure based densities are equal for two hemispheres at a time where one was by large more active than the other, seems to support this hypothesis.

## 6. Conclusions

From the analysis of the observational data presented here, several conclusions can be drawn. First of all, the upper transition region of II Peg was in a phase of low activity when the observing programme was carried out. The transition region fluxes measured are amongst the lowest ever found in this system and no trace of rotational modulation of the ultraviolet emission is apparent. While the low activity affects mainly the upper transition region, lines originated in lower temperature regime such as C II and the essentially chromospheric Mg II lines are less affected. The low activity seems to contradict the fact found from the photometric light curve that in this epoch there was a relatively high global coverage by starspots (see Paper I). It should be noted that this discussion applies to the quiescent state of II Peg during the first weeks after one of the most energetic flares detected in this system. No rotational modulation is detected in any of the lines observed with *IUE* except Fe II and even in this case, the evidence is weak.

The comparison of the observations presented here with the previous observing campaigns shows no hints of cyclic behaviour in the C IV emission. It nevertheless suggests the possibility that the minimum flux within each observing campaign diminishes. The latest observations obtained with *HST* consist only of two spectra and are therefore of no help in order to check if the trend continues after 1992.

New emission measure distributions presented here differ from previous determinations mainly due to the decrease in the upper transition region line fluxes (Si IV, C IV and N V). Therefore we find a steeper decrease in the slope of the high temperature range of the emission measure distribution.

The Si III] density diagnostic gives a value of the electron density during quiescence around  $\log N_e = 11.6\pm 0.25$  in agreement with previous work. The enhancement of the density during the flare can only be assessed with the second spectrum (SWP 45532) and amounts to 0.3 dex.

The Si IV( $\lambda\lambda$ 1394/1403)/C III]( $\lambda$ 1909) line ratio, characteristic of a higher temperature range, yields values of  $\log N_e = 10.7$ , 10.9 and 11.2 for the mean quiescent state and the two flare spectra respectively. As shown by Fig. 3 in Paper I, the light curve of the flare has a complex time development which makes it difficult to interpret integrated observations as the SWP spectra used in the density determination.

*Acknowledgements.* LMS thanks PBB for giving him the chance to fulfill the dream of working in astronomy and the ever-lasting treasure of the memory of his friendship. In memoriam. Research at Armagh Observatory is supported by a Grant-in-Aid from the Department of Education of Northern Ireland. This research utilised software and hardware provided by the UK SERC STARLINK computing network. LMS acknowledges support from the European Community's COM-MET grant.

## References

- Anders E., Grevesse N., 1989, *Geochimica et Cosmochimica Acta* 53, 197
- Andrews A.D., Rodonó M., Linsky J.L., et al., 1988, *A&A* 204, 177
- Arnaud M., Rothenflug R., 1985, *A&A* 60, 425
- Ayres T.R., 1990, *PASP* 102, 1420
- Ayres T.R., Simon T., Stern R.A., et al., 1998, *ApJ* 496, 428
- Baluja K.L., Burke P.G., Kingston A.E., 1980, *J. Phys. B* 13, L543
- Baluja K.L., Burke P.G., Kingston A.E., 1981, *J. Phys. B* 14, 1333
- Boggess A., Wilson R., 1987, *Understanding the Universe with the IUE Satellite*, D. Reidel
- Brekke P., 1993, *ApJS* 87, 443
- Byrne P.B., 1992a In: Byrne P.B., Mullan D.J. (eds.) *Surface Inhomogeneities on Late-type Stars*, publisher = Springer
- Byrne P.B., 1992b, In: Thomas J.H., Weiss N.O. (eds.) *The Theory of Sunspots*, Kluwer, Dordrecht
- Byrne P.B., 1996, In: Greiner J., Gershberg R.E. (eds.) *Flares and Flashes*, Kluwer, Dordrecht
- Byrne P.B., Doyle J.G., Brown A., Linsky J.L., Rodonó M., 1987, *A&A* 180, 172
- Byrne P.B., Panagi P.M., Doyle J.G., et al., 1989, *A&A* 214, 238
- Byrne P.B., Panagi P., Lanzafame A.C., et al., 1995, *A&A* 299, 115
- Byrne P.B., Abdul Aziz H., Amado P.J., et al., 1998, *A&AS* 127, 505
- Cochrane D.M., McWhirter R.W.P., 1983, *Phys. Scr.* 28, 25
- Doschek G.A., Feldman U., van Hoosier M.E., Bartoe J.-D., 1976, *ApJS* 31, 417
- Doyle J.G., 1988, *A&A* 192, 281
- Doyle J.G., Butler C.J., Byrne P.B. et al., 1989a, *A&A* 223, 219
- Doyle J.G., Byrne P.B., van den Oord G.H.J., 1989b, *A&A* 224, 153-161
- Doyle J.G., Kellett B.J., Butler C.J. et al., 1992a, *A&AS* 96, 351
- Doyle J.G., van den Oord G.H.J., Kellett B.J., 1992b, *A&A* 262, 533
- Doyle J.G., Mathioudakis M., Murphy H.M., Avgoloupis S., Mavridis L.N. and Seiradakis J.S., 1993, *A&A*, 278, 499
- Dufton P.L., Kingston A.E., 1985, *ApJ* 289, 844
- Griffiths N.W., Jordan C., 1998, *ApJ* 497, 883-895
- Hayes, M. A. and Nussbaumer, H., 1984, *A&A* 134, 193
- Jordan C., Ayres T.R., Brown A., Linsky J.L., Simon T., 1987, *MNRAS* 225, 903
- Lennon D.J., Dufton P.L., Hibbert A., Kingston A.E., 1985, *ApJ* 294, 200
- Linsky J.L., Wood B.E., Judge P., et al., 1995, *ApJ* 442, 381
- Mendoza C.J., 1981, *Phys. B* 2645
- Mewe R., Kaanstra J.S., van den Oord G.H.J., Vink, J., Tawara Y., 1997, *A&A* 320, 147
- Nichols J.S., Linsky J.L., 1996, *AJ* 111, 517
- Phillips K.J.H., Bromage G.E., Doyle J.G., 1992, *ApJ* 385, 731
- Rodonó M., Byrne P.B., Neff J.E., et al., 1987, *A&A* 176, 284
- Vogt S.S., 1981, *ApJ* 247, 975
- Wood B.E., Harper G.M., Linsky J.L., Dempsey R.C., 1996, *ApJ* 458, 761
- Wood B.E., Linsky J.L., Ayres T.R., 1997, *ApJ* 478, 745